Journal of Luminescence 130 (2010) 415–423

Contents lists available at ScienceDirect

Journal of Luminescence

journal homepage: www.elsevier.com/locate/jlumin

Study of solvent-conjugated polymer interactions by polarized spectroscopy: MEH–PPV and Poly(9,9′-dioctylfluorene-2,7-diyl)

Rafael F. Cossiello [a], Mariano D. Susman [b], Pedro F. Aramendía [b,*], Teresa D.Z. Atvars [a,*]

[a] Universidade Estadual de Campinas, Instituto de Química, Caixa Postal 6154, Campinas, 13084-971 SP, Brazil
[b] INQUIMAE and Departamento de Química Inorgánica, Analítica y Química Física, Facultad de Ciencias Exactas y Naturales, Universidad de Buenos Aires, Pabellón 2, Ciudad Universitaria, C1428EHA, Buenos Aires, Argentina

ARTICLE INFO

Article history:
Received 3 April 2009
Received in revised form
6 October 2009
Accepted 19 October 2009
Available online 27 October 2009

Keywords:
Fluorescence anisotropy
Solvent effects
Solutions and films
Conjugated polymers
Polyfluorene
MEH–PPV

ABSTRACT

Absorption, emission, and anisotropy measurements were performed on poly-[2-methoxy-5(2′-ethylhexyloxy)–1,4-phenylenevinylene] (MEH–PPV) and poly-(9,9′-dioctylfluorene-2,7-diyl) (PF) solutions of various solvents, and in thin films deposited from them. The good correlation of MEH–PPV absorption and emission energy with Hildebrandt's dispersive parameter indicate that dispersive forces regulate the effective extent of the luminophore. The excitation and the emission spectra of α and β chains can be distinguished in PF solutions using the steady-state anisotropy. PF films show greater memory effect from the solutions from which they were spun than MEH–PPV. Anisotropy of MEH–PPV is very low, both in solutions and in films reflecting efficient energy migration. Anisotropy of PF in solutions and films demonstrates great differences in energy transfer efficiency within the α and β phases, while there is no energy transfer between these chain conformations.

1. Introduction

Conjugated polymers attracted much attention in the last thirty years since the discovery of the electron conductivity of poly(acetylene) and later of poly(aniline) and several other polymers and copolymers [1,2]. More recently, during the nineties, the scientific and technological interests were renewed by the discovery of the electroluminescence of conjugated polymers and copolymers [2].

These conjugated polymers are materials with a great variety of chemical structures, synthesized by distinct procedures, with multiple functionalities conferring different colors to operating devices, from violet to red [3–14]. Each one of these particular chemical structures may have distinct physical, chemical and electrical properties. In addition, because of the lower melting point (in the case of semicrystalline materials) and lower glass transition temperature compared to inorganic semiconductors, the conjugated electroluminescent polymers can easily be processed and thin films can be prepared by in situ polymerization or by deposition on a substrate using spin coating, self assembly, dip coating and casting [1]. The facility to process organic polymers has, on the other hand, various morphological consequences such as the presence of defects, stress, non-uniform thickness, etc, that greatly lower electrical and electroluminescence performance [10–31].

There are several experimental techniques useful in studies of macromolecular chain conformations: scanning electron microscopy, atomic force microscopy, small angle X-ray scattering and wide angle X-ray diffraction [26,27], near-field optical microscopy [24,25,29], confocal microscopy and single molecule spectroscopy [32–34], optical microscopy, and luminescence spectroscopy [32–35]. In particular, the steady-state photoluminescence anisotropy provides information on molecular conformation and reorientation during the lifetime of the excited sate [35–43].

In multiple chromophoric systems, such as conjugated polymers, the excitation energy can be converted to fluorescence emission whose anisotropy depends strongly on the chain conformational relaxation, on the energy transfer processes and on the energy migration probability. In general, when the energy migration is faster than the emission decay, a strong depolarization of the fluorescence takes place [36–43].

Film morphology depends on several processing parameters [17–29,43,44], but it is particularly influenced by the solvent used. Polymer chains form coils in unfavorable solvents to minimize their exposure to the solvent and this has a strong impact on its photophysical properties [23,31,33,36,45–47]. For example, the excimer emission can be enhanced in poor solvents while it is minimized in good solvents that induce a more extended conformation [48,49]. The reason for the changes in

* Corresponding authors. Tel.: +55 19 35214729.
E-mail addresses: pedro@qi.fcen.uba.ar (P.F. Aramendía), tatvars@iqm.unicamp.br (T.D.F. Atvars).

0022-2313/$ - see front matter © 2009 Published by Elsevier B.V.
doi:10.1016/j.jlumin.2009.10.006

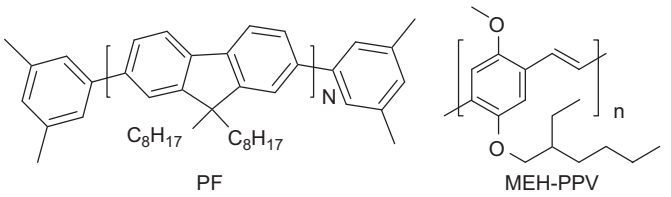

Fig. 1. Chemical structures of poly-(9,9′-dioctylfluorenyl-2,7-diyl)-end capped with dimethyl phenylene (PF) and poly-[2-methoxy-5-(2′-ethylhexyloxy)-*p*-phenylene-vinylene] (MEH–PPV).

photo and electroluminescence properties in films prepared from different solvents is that a part of the conformation in solution should be maintained in the solid state, which is called the memory effect [30–34].

Hildebrand solubility parameter is often used to quantify polymer–solvent interactions either in the global form or through its specific components that describe the hydrogen bonding interaction (δ_H), the dipolar interactions (δ_p) and the dispersive interactions (δ_d) [50–53]. These components account better for specific polymer–solvent interactions. For example, although toluene ($\delta = 18.2\ J^{1/2}\,cm^{-3/2}$) and ethyl acetate ($\delta = 18.2\ J^{1/2}\,cm^{-3/2}$) have the same Hildebrand solubility parameters, their components (δ_H, δ_d, δ_p) are different as well as their solvation ability for poly-[2-methoxy-5(2′-ethylhexyloxy)–1,4-phenylenevinylene] (MEH–PPV) [46].

The knowledge of the solvation ability is particularly important when multi-layer electroluminescent devices are desirable. Here the morphology of one layer must be maintained during the deposition of the subsequent layers; a condition that requires a good solvent for one material and a poor solvent for the other. Therefore, in the present work we explore the applicability of the Hildebrand parameter to discuss the behavior of MEH–PPV and poly-(9,9′-dioctylfluorene-2,7-diyl) (PF) (Fig. 1) in solutions of toluene, chloroform, dichloromethane, tetrahydrofuran (THF), ethyl acetate, dimethylsulfoxide (DMSO), and acetonitrile and the consequence of the solvent–polymer interaction on the photoluminescence features of polymers in solution and in films deposited from different solvents. To analyze the solvent quality we use the steady-state spectroscopy and fluorescence anisotropy measurements in both dilute polymer solutions and thin films prepared by dip or spin coating. Differences in photoluminescence spectra and in fluorescence anisotropy are discussed in terms of the chain conformation in solution and in films, and their implications for energy migration and transfer.

2. Experimental section

2.1. Materials

End capped poly-(9,9′-dioctylfluorenyl-2,7-diyl) (PF) $M_w \sim 40-120\,kg\,mol^{1-}$ was purchased from ADS Inc. and poly-[2-methoxy-5-(2′-ethylhexyloxy)-p-phenylene-vinylene] $M_w = 181\,kg\,mol^{1-}$ (MEH–PPV), from Sigma-Aldrich. They were used as received. Dichloromethane (Merck 98% and Carlo Erba, Analytical grade), toluene (Merck 98% and Merck, spectroscopical grade) were fractionally distilled before use, chloroform (Labsynth 99.8%). THF (Merck 98.5% or Aldrich ACS—99+%) was distilled with Na at reduced pressure, ethyl acetate (Merck 99% and EM Science ACS, for HPLC), DMSO (Merck 98%), and acetonitrile (Merck 99%) were dried before use.

Polymer solutions in each solvent were prepared by dissolving the solid polymer under stirring, during several hours in the dark under mild heating until complete dissolution. All solutions were maintained in dark in a sealed flask. Samples of thin films were prepared by dip coating or by spin coating of poly(ethylene terephthalate) (PET) slices ($1 \times 2 \times 0.5$ cm) into the polymer solutions. Samples were dried for 2 h at room temperature after dipping to remove residual solvent.

2.2. Methods

Electronic absorption spectra were recorded in a Hewlett–Packard-8452A UV–vis spectrometer. When necessary, polarized absorption was detected by placing film polarizers before and after the sample. Each polarized spectrum is referenced to the baseline obtained with the corresponding orientation of the polarizer. The steady-state fluorescence spectroscopy was performed on a PC1 photon counting spectrofluorimeter from ISS Inc. or on a PTI quantamaster spectrofluorometer. Slits were selected for a spectral resolution between 4 and 8 nm in excitation and in emission. For fluorescence emission and excitation spectra of solutions, a square quartz cuvette, 1 cm side, was employed. Spectra of films were recorded in a back-face configuration to diminish stray light reaching the detector.

Fluorescence anisotropy was measured using a couple of film polarizers on the excitation and emission beams in either of the spectrofluorimeters operating in a L-format. The fluorescence anisotropy is calculated according to Eq. (1), where I is the fluorescence intensity at one specific wavelength and "v" and "h" are the relative orientation of the polarizers, denoting perpendicular and on the plane of incidence, respectively. The first letter of the subscript represents the orientation of the excitation polarizer and the second that of the emission polarizer [54]:

$$r(\lambda) = \frac{I_{vv} - GI_{vh}}{I_{vv} + 2GI_{vh}} \quad (1)$$

where I_{vv} and I_{vh} are the spectral intensity determined using the polarizer and the analyzer in vertical positions and with the polarizer in the vertical and the analyzer in the horizontal position, respectively. $\boldsymbol{G}$ is a correction factor of instrumental response given by Eq. (2):

$$G(\lambda em) = \frac{I_{hv}(\lambda em)}{I_{hh}(\lambda em)} \quad (2)$$

where I_{hv} and I_{hh} are the spectra recorded with polarizer in horizontal position in both cases, and the analyzer in vertical and horizontal positions, respectively [54].

3. Results

3.1. Fluorescence spectra and anisotropy of MEH–PPV in solutions

The electronic absorption spectra of MEH–PV in 18 mg L^{-1} solutions (see Fig. 2) show broad absorption bands. Broad absorption spectra of conjugated polymers result of the convolution of electronic transitions from macromolecular segments of different conjugation lengths overlapped with several vibronic states [2–25,32–34,55–57].

Absorption spectra of MEH–PPV in acetonitrile, DMSO and ethyl acetate are different from those in other solvents (Fig. 2a). The lower solubility of MEH–PPV in these solvents and, consequently, the lower concentration in solution leads to a weak absorbance (less than 0.1). Concentration in these cases are smaller than 18 mg L^{-1}. The absorption bands are centered at 425 nm for acetonitrile, 480 nm for ethyl acetate and DMSO, 492 nm for THF and 496 nm for chloroform and toluene.

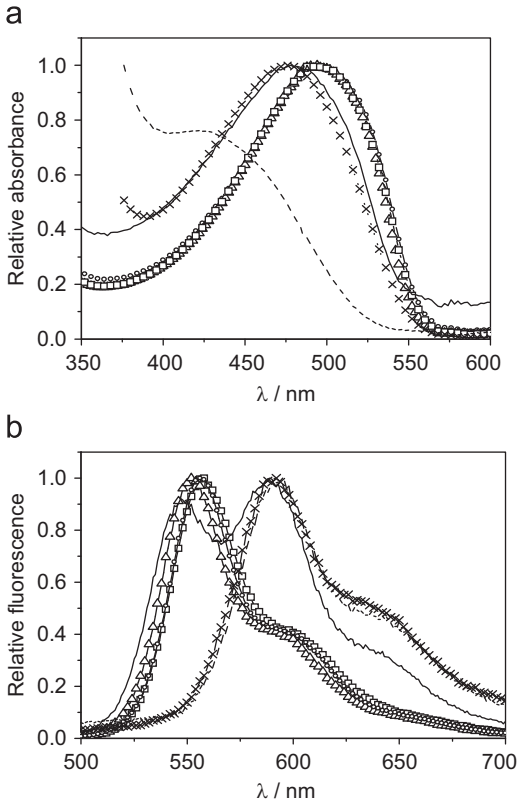

Fig. 2. (a) Relative absorption and (b) relative fluorescence spectra (λ_{exc}=495 nm) of MEH–PPV in solution of: —, ethyl acetate; -□-□-, chloroform; -△-△-, THF; -○-○-, toluene; (these later three spectra almost overlap in absorption and in emission), -×-×-, DMSO; and - - -. acetonitrile. Polymer concentration was 18 mg L^{-1} except in ethyl acetate, acetonitrile and DMSO (see text).

The MEH–PPV fluorescence emission spectra of 18 mg L^{-1} solutions (Fig. 2b) show that in good solvents (toluene, chloroform and THF) the emission maximum is centered at λ_{em}=555 nm, with shoulders at 600 and 650 nm, corresponding to a vibronic progression originated on the C–C vibrational stretching modes of aromatic rings. A very small blue shift is observed in THF (λ_{em}=552 nm) when compared to toluene solutions, which can be attributed to solvatochromic effects, in agreement with previous observations in THF and chlorobenzene [31]. There is a pronounced spectral red-shift of the emission spectra (λ_{em}=592 nm) for MEH–PPV in poor solvents (DMSO and acetonitrile) with a complete absence of higher energy emission band. This result is explained by MEH–PPV aggregation [20,22,25,28,29,31,37,46]. Distinctly from both previous solvent sets, the spectrum in ethyl acetate shows two prominent bands; a higher energy band slightly blue-shifted, λ_{em}=552 nm, compared to good solvents and a lower energy band with maximum at λ_{em}=590 nm comparable to that observed in poor solvents. In all cases, it is worth noting that the fluorescence emission is not the mirror image of the absorption spectrum, indicating that distinct sites are absorbing and emitting [20,22,25,28,29,31,37,46].

The steady-state fluorescence emission of MEH–PPV in dilute solutions of good solvents is attributed to the intrachain exciton being composed by three vibronic bands appearing at 564, 599 and 632 nm [23,24,29–31,33,46]. The larger apparent Stokes shift originates from conformational relaxation, energy migration or energy transfer processes, as usually observed for conjugated polymers [38–42]. The relative intensity of these bands depends on the electron-phonon coupling, on the macromolecular conformation relaxation, and on the presence of aggregates that

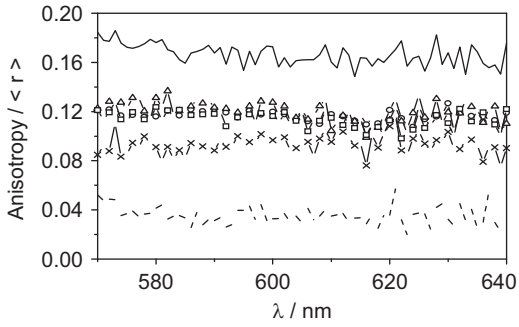

Fig. 3. Fluorescence anisotropy (λ_{exc}=495 nm), $\langle r \rangle$ of MEH–PPV in dilute solutions of—ethyl acetate, -□-□-, chloroform; -△-△-, THF; -○-○-, toluene; -×-×-, DMSO; and - - -, acetonitrile. Polymer concentration as in Fig. 2.

usually emit at the red-edge of the intrachain species [23,25,29–31,33,46]. Therefore, in the absence of aggregates, even for good solvents, the band profile is not expected to be the same [23,25,29–31,33,46]. This can explain slight differences between the emission spectra in good solvents while in these same environments the absorption spectra remain practically the same. The emission spectrum of MEH–PPV in ethyl acetate presents two bands, the higher energy attributed to the intrachain exciton (isolate chains) and the lower energy attributed to the interchain exciton (aggregate involving more than one macromolecular segment). In poor solvents, such as acetonitrile and DMSO, only the emission of aggregates is observed. In other words, in good solvents the conformation of polymeric chains is more extended and the interchain interactions, i.e. π–π stacking, are minimized by the solvation layer, while in poor solvents interchain interactions or coil conformation favoring intersegmental interactions increase the probability of aggregation [25,32,35,48,49].

We also found that the steady-state emission anisotropy, $\langle r \rangle$, of MEH–PPV in these five solutions (Fig. 3, Table 1) is independent of the emission wavelength and has distinct values for three types of solvents (as classified above): $\langle r \rangle$=0.114 in chloroform, $\langle r \rangle$=0.116 in toluene and $\langle r \rangle$=0.120 in THF (good solvents); $\langle r \rangle$=0.166 in ethyl acetate (solvent with intermediate quality), and $\langle r \rangle$=0.093 in DMSO and $\langle r \rangle$=0.035 in acetonitrile (poor solvents). Transient measurements have shown that immediately after excitation MEH–PPV anisotropy in dilute chlorobenzene solution is r_0=0.4, the theoretically maximum value, and then the value decreases to r=0.15 with a characteristic lifetime of 20 ps and to r=0.08 at longer times (limiting anisotropy, r_∞) [54]. Considering an excited state lifetime of 250 ps, the above values render $\langle r \rangle$=0.11, in good agreement with our results ($\langle r \rangle = r_0\tau_r/(\tau_r+\tau_f)+r_\infty$; where τ_r is the characteristic time for the anisotropy decay and τ_f is the excited state lifetime). In THF solution, the anisotropy of MEH–PPV was measured to decrease from 0.4 to r=0.18–0.20 with a characteristic lifetime of 150 ps [31], considering the reported excited state lifetime of 300 ps, a value of $\langle r \rangle \approx 0.13$ can be calculated, also in good agreement with our results.

3.2. Fluorescence spectra and anisotropy of MEH–PPV films

The steady-state fluorescence spectra of MEH–PPV thin films deposited on PET surface by dip coating from solutions of different solvents (Fig. 4) are red-shifted (λ_{em} (THF)=587 nm, λ_{em} (chloroform)=588 nm and λ_{em} (toluene)=600 nm) compared to dilute solutions of good solvents and ethyl acetate. We were not able to prepare films from DMSO and acetonitrile solutions due to the low MEH–PPV solubility. The emission spectra of films are very similar to those observed in solution of poor solvents (Fig. 2), confirming that in solution of acetonitrile and

Table 1
The steady-state anisotropy of MEH–PPV and PF in different solvents (subscript *s*) and of thin films (subscript *f*) spun from solutions with the same solvents.

	$\langle r\rangle_s$ (MEH–PPV)	$\langle r\rangle_s$ (PF)		$\langle r\rangle_f$ (MEH–PPV)	$\langle r\rangle_f$ (PF)
		α band	β band		
Ethyl acetate	0.166 ± 0.008	0.05 ± 0.01	0.30 ± 0.05	0.02 ± 0.01	nd
Chloroform	0.114 ± 0.006	0.05 ± 0.01[a]	0.30 ± 0.05[a]	0.04 ± 0.01	0.03 ± 0.01[a]
Toluene	0.116 ± 0.005	0.125 ± 0.005	0.35 ± 0.01	0.07 ± 0.01	0.06 ± 0.02
THF	0.120 ± 0.008	0.130 ± 0.005	0.26 ± 0.01	0.01 ± 0.01	0.04 ± 0.01
DMSO	0.093 ± 0.008	nd	nd	nd	Nd
Acetonitrile	0.035 ± 0.007	nd	nd	nd	nd

nd: not determined.

[a] Values in dichloromethane.

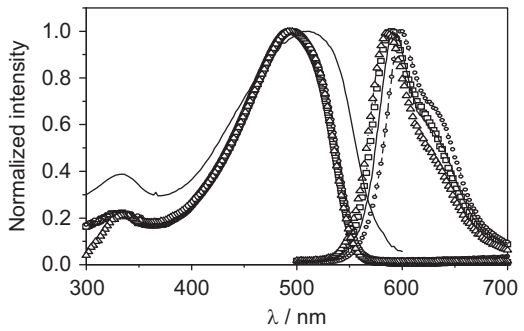

Fig. 4. Normalized fluorescence excitation (λ_{em}=600 nm) and emission (λ_{exc}=495 nm) spectra of MEH–PPV films prepared by dip coating from solutions in—ethyl acetate, -□-□-, chloroform; -△-△-, THF; and -o-o-, toluene.

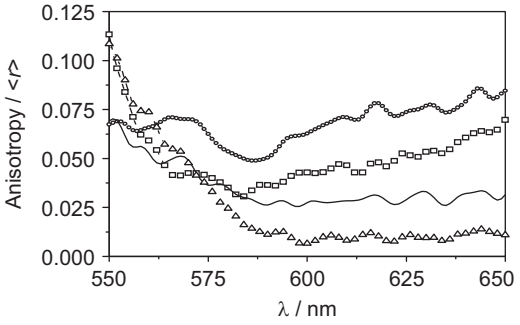

Fig. 5. Fluorescence anisotropy (λ_{exc}=495 nm), $\langle r\rangle$, of MEH–PPV in films spun from solutions of —,ethyl acetate; —, chloroform; -△-△-, THF; and -○-○-, toluene.

DMSO the emission is originated from interchain or intersegmental species. As already observed, the emission of MEH–PPV films is not the mirror image of the excitation spectrum because the system undergoes a fast energy migration from the absorbing luminophores towards the lower emissive center in addition to the conformational relaxation processes, which are expected to play a minor role in the solid state. Due to these processes there is a large apparent Stokes shift between emission and excitation spectra [17–23,29,33,34,56].

There are several reasons for both red-shift and differences in the intensity ratio of vibronic bands when MEH–PPV films are spun from different solutions: the spectral red-shift can be produced by inner filter effect usually observed for thick or concentrated samples [54]. It can also be attributed to chain conformation. Because these are very thin films, the absorbance is low, and there is a great spectral shift between absorption and emission, chain conformation and its distribution is responsible for different emission spectra.

Morphology of MEH–PPV films has been studied by several high-resolution techniques such as near-field scanning optical microscopy, transmission electron microscopy, wide angle X-ray scattering, polarized optical microscopy [24,26,28,29,35] and single molecule spectroscopy [32–34]. It is accepted that MEH–PPV films have a low degree of crystallinity although in the film short-range chain packing domains are built in the nanometric scale consistent with the emission of aggregated forms [20,24].

The steady-state fluorescence anisotropies of MEH–PPPV films spun from solutions of different solvents are: $\langle r\rangle$=0.07 for toluene, $\langle r\rangle$=0.04 for chloroform, $\langle r\rangle$=0.02 for ethyl acetate and $\langle r\rangle$=0.01 for THF (Fig. 5, Table 1). These values are the average in the 575–650 nm range where emission intensity is appreciable. MEH–PPV anisotropy values are one order of magnitude smaller than in solution indicating that fluorescence depolarization regardless its mechanism (energy migration, energy transfer processes or the highly unlikely conformational relaxation) are more efficient in solid state than in dilute solutions.

3.3. Fluorescence spectra and anisotropy of PF in solutions

The electronic absorption spectra of PF were recorded in solutions (0.50 g L^{-1}) of toluene, chloroform, THF, acetonitrile, ethyl acetate and DMSO (Fig. 6a). In toluene, chloroform, THF and DMSO solutions the absorption band is broad and centered at around 390 nm. This band is attributed to the α-backbone conformations, which is disordered and usually observed in solutions and in thermally stabilized films [13,14,41–43,58–60]. A small red-shift is observed for THF and DMSO solutions (λ_{abs}=394 nm). The electronic absorption band of PF in acetonitrile solution is broader with a higher intensity peak centered at 383 nm, a shoulder at the red-edge (402 nm) and a lower intensity sharper band at 436 nm. This band appears with low intensity in the other PF solutions. The absorption spectrum of PF in ethyl acetate solutions is quite different from other solvents. There is a splitting of the absorption band in a higher energy component with a lower intensity centered at 387 nm and a higher intensity component at its red-edge (405 nm) in addition to the lower intensity band at 436 nm. This lowest energy band is also relatively more intense than in other solvents. This spectrum can be considered as an overlap of two absorptions; from the luminophores in chains with the α-conformations as in toluene, chloroform, THF and DMSO and in chains with the β conformations absorbing at the red-edge. It has been proposed that the 0–0 vibronic band at 436 nm corresponds to the luminophores of polyfluorenes in β conformations with other vibronic components overlapped with the higher energy band of α-conformers [13,14,41–43,58–60]. The β conformations have more planar polymer backbone [13,14,41–43,58–60]. In

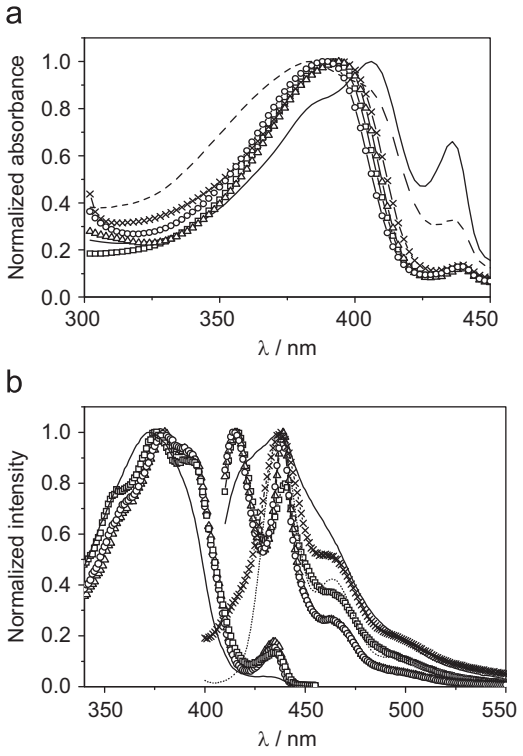

Fig. 6. (a) Normalized absoption and (b) fluorescence excitation and emission spectra of PF in solutions of —, ethyl acetate; -□-□-, dichloromethane; -△-△-, THF; -○-○-, toluene; - × - × -, DMSO; and **- - -**, acetonitrile. For emission, λ_{exc}=395 or 400 nm. For excitation, λ_{em}=465 nm.

conclusion, based on the electronic absorption spectra, toluene, chloroform, THF, and DMSO are good solvents for PF but even for these solvents there is a low concentration of chains ordered as in the β phase. In poor solvents (ethyl acetate) there is a larger amount of chains in the β phase, while in acetonitrile there is a mixture of isolated luminophores and a relative high concentration of segments ordered as in the β phase.

Fluorescence emission and excitation spectra were recorded in solutions of THF, toluene, dichloromethane and ethyl acetate at a concentration of 0.18 g L^{-1} and are displayed in Fig. 6b. Excitation spectra are slightly wavelength-dependent in all cases, and are different from the absorption spectra (excitation spectra recorded at three different emission wavelengths, λ_{em}=415, 440 and 465 nm, are shown in Fig. 1 in Supporting Information). Considering that there are two emitting species, the appointed differences can be attributed to different emission yields or relative absorption of α and β phases.

Fluorescence emission spectra of the PF solutions (THF, dichloromethane, toluene and ethyl acetate) were also recorded for excitation wavelengths from λ_{exc}=380–430 nm (Supporting Information—Fig. 2). The dependence of the emission spectra with excitation wavelength is more pronounced. Upon excitation wavelength increase, the maximum corresponding to the α phase decreases relative to the maximum around 438 nm, and the band structure becomes more pronounced. In ethyl acetate, which shows a poorly resolved band emission structure at excitation wavelength below 400 nm, clearly resolved bands are displayed when excitation is performed above 410 nm, similar to other solvents [13,14,41,42,58]. In addition, the relative intensity of the lower energy emission bands (465 and 500 nm) become higher for excitation at the red-edge of the excitation band ($\lambda_{exc} > 415$ nm) indicating that although in a lower concentration, that species is present even in good solvents.

It is note worthy that while PF absorption spectrum in DMSO solutions is similar to those in good solvents, the emission is similar to poor solvents. The emission spectra of PF in acetonitrile show the spectral features typical of the β-chain conformation. The 0–0 phonon band (λ_{em}=438 nm) seems to be a mirror image of the lower energy absorption band (the 0–0 absorption band at 436 nm). This behavior has been already reported for the β-phase emission spectrum, which exhibits a sharper profile, a smaller Stokes shift and a more resolved vibronic structure [61].

The discussion of the solvent quality for PF can be done in the same terms as we did for MEH–PPV. Based on the Hildebrand solubility parameters THF, chloroform, dichloromethane and toluene are good solvents for PF; DMSO has an intermediate quality character while ethyl acetate and acetonitrile are poor solvents. Therefore, we can say that good solvents for PF should have dispersive and dipolar components in the range $16.8 \leq \delta_d \leq 18.0\ J^{1/2}\ cm^{-3/2}$ and $1.4 \leq \delta_p \leq 5.7\ J^{1/2}\ cm^{-3/2}$, respectively. Because DMSO has the dispersive component (δ_d=18.4 $J^{1/2}$ $cm^{-3/2}$) near the limit of the ideal range and a larger dipolar (δ_p=16.4 $J^{1/2}$ $cm^{-3/2}$) component, it behaves as a solvent with intermediate quality. On the other hand, for acetonitrile (a poor solvent) the δ_d=15.3 $J^{1/2}$ $cm^{-3/2}$ present a low value, while the dipolar component is much larger (δ_p=18.0 $J^{1/2}$ $cm^{-3/2}$); for ethyl acetate (also a poor solvent) the δ_d=15.8 $J^{1/2}$ $cm^{-3/2}$ shows low value, while the dipolar component is within the adequate range (δ_p=5.3 $J^{1/2}$ $cm^{-3/2}$). Taking all together we can say that the most important component controlling the PF solubility is the dispersive interactions. According to the experimental range of Hansen's solubility [50–53], we can estimate the solubility parameters of PF as δ_d=18.5 $J^{1/2}$ $cm^{-3/2}$, δ_p=2.0 $J^{1/2}$ $cm^{-3/2}$ and δ_H= 1.0 $J^{1/2}$ $cm^{-3/2}$, with a global parameter about δ_d=18.6 $J^{1/2}$ $cm^{-3/2}$. Again, the global Hildebrand solubility parameter cannot explain the solubility ordering of ethyl acetate since it has similar solubility parameter, although the photophysical behavior of the solution is completely different.

The steady-state fluorescence anisotropy was also determined for PF in solutions (Fig. 7, Table 1). The steady-state anisotropy strongly depends on excitation and emission wavelengths. The general features of the dependence of anisotropy with wavelength are similar in all four solvents. THF and toluene are shown in Fig. 7, as an example (similar spectra in dichloromethane and in ethyl acetate are shown in Fig. 3 of the Supporting Information). The steady-state anisotropy increases with excitation wavelength almost in the same way irrespective of whether it is detected in the second emission band (typically around 440 nm) or in the emission shoulder around 465 nm. The maximum value of the anisotropy is reached in all cases in the excitation band corresponding to the β phase (420–440 nm). Values as high as 0.35 are measured in toluene and in ethyl acetate for this band. This indicates absence of depolarization effects such as torsional motions or energy transfer. In the UV edge of the excitation band, the value of the steady-state anisotropy is close to 0.1 in all cases. This indicates a great depolarization.

On the other hand, the steady-state emission anisotropy shows very different values and wavelength dependence when the samples are excited at 400 nm, corresponding mainly to the absorption of the isolated luminophores, than when they are excited at around 435 nm, in the maximum corresponding to the β phase. In the first case, a low anisotropy is observed with slight maxima coinciding with the emission maxima at around 440 and 465 nm. When excitation is performed at 435 nm, the values of the steady-state anisotropy are higher and show an increase in the tendency with wavelength.

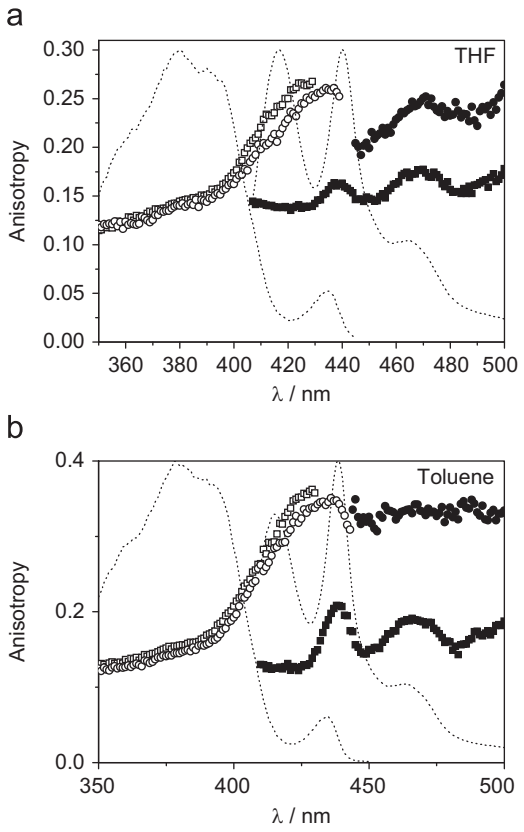

Fig. 7. The steady-state anisotropy of PF solutions in THF and toluene. Dotted lines correspond to excitation (λ_{em}=465 nm) and emission (λ_{exc}=400 nm) spectra. Scatter points represent the steady-state anisotropy in the excitation spectra, λ_{em}=464 nm (empty squares) and λ_{em}=437 nm (empty circles), and in the emission spectra, λ_{exc}=400 nm (full squares) and λ_{exc}=434 nm (full circles).

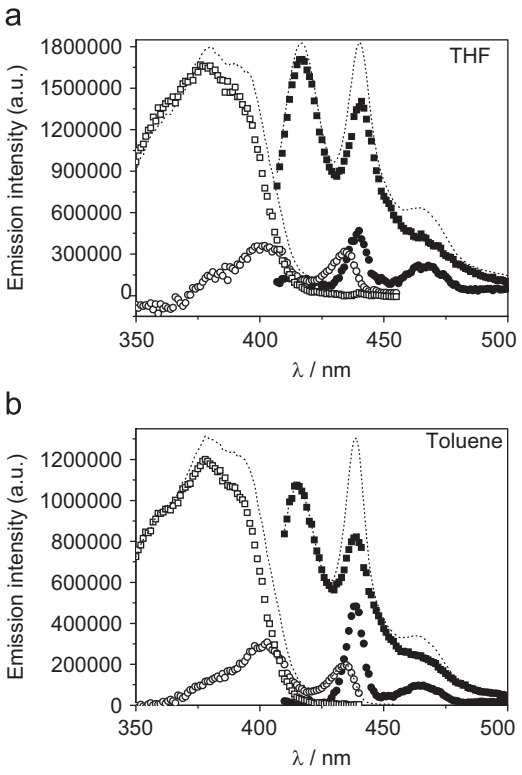

Fig. 8. Spectral deconvolution of excitation and emission spectra of PF in solution of THF and toluene. Dotted lines correspond to total excitation (λ_{em}=465 nm) and emission (λ_{exc}=400 nm) spectra. Points correspond to the components of the α phase (hollow squares, excitation, and full squares, emission, f_1, see text and Eqs. (3)–(5)) and the β phase (hollow circles, excitation, and full circles, emission, f_2, see text and Eqs. (3)–(5)).

Results are compatible with homo energy transfer between isolated luminophores being the main depolarization pathway.

Taking into account that anisotropy is additive and that there are at least two species responsible for the emission, we can write

$$\langle r\rangle = r_1 f_1 + r_2 f_2 \tag{3}$$

$$f_1 + f_2 = 1 \tag{4}$$

In the previous equations, f_i are the fractions of the emission intensity corresponding to each species, and r_i are their respective steady-state anisotropies, which, for the following calculations, will be considered to be wavelength-independent in the excitation and emission wavelength ranges measured.

Eqs. (3) and (4) can be solved for the intensities of each component, thus allowing calculation of their emission and excitation spectra

$$I_1 = I_t f_1 = \frac{\langle r\rangle - r_2}{r_1 - r_2},$$
$$I_2 = I_t - I_1 = I_t f_2 = \frac{r_1 - \langle r\rangle}{r_1 - r_2} \tag{5}$$

Arbitrarily we identify 1 with the β phase and 2 with the α phase. The deconvoluted spectra are shown in Fig. 8 for the case of THF and toluene. Values of r_1 and of r_2 are listed in Table 1.

For the isolated luminophore of PF in solution the anisotropy is low. Reported values of $\langle r\rangle$=0.096 ($\lambda_{exc} < 380$ nm) measured for poly[9,9-di(ethylhexyl)fluorene] in methylcyclohexane dilute solution [44] and $\langle r\rangle$=0.10 for PF in methylcyclohexane solution [45], are in line with our measurements. On the other hand, the β phase displays very high anisotropy, indicating that hardly any depolarization occurs once excitation energy reaches this center.

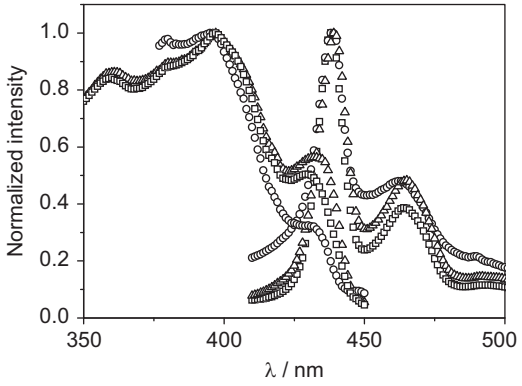

Fig. 9. Fluorescence excitation (λ_{em}=465 nm) and emission (λ_{exc}=400 nm) spectra of PF films spun from solutions of: -□-□-, dichloromethane; -△-△-, THF -○-○- toluene.

3.4. Fluorescence spectra and anisotropy of PF films

The fluorescence excitation and emission spectra of PF spun from solutions of toluene, dichloromethane and THF are shown in Fig. 9. Excitation spectra show differences in the relative contributions of β-phase components, these decrease the

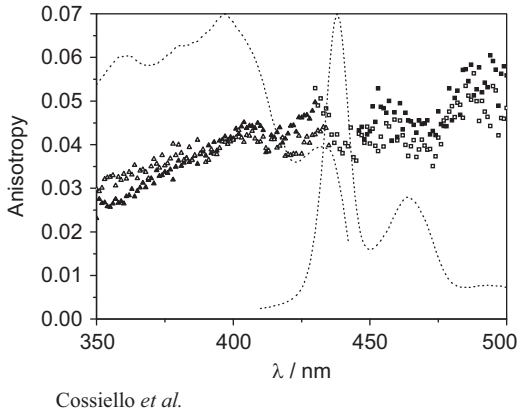

Fig. 10. The steady-state anisotropy of PF films spun from THF solution. Dotted lines correspond to total excitation (λ_{em}=465 nm) and emission (λ_{exc}=400 nm) spectra. Points represent the steady-state anisotropy in the excitation spectra, λ_{em}=464 nm (hollow triangles) and λ_{em}=437 nm (full triangles), and in the emission spectra, λ_{exc}=400 nm (hollow squares) and λ_{exc}=434 nm (full squares).

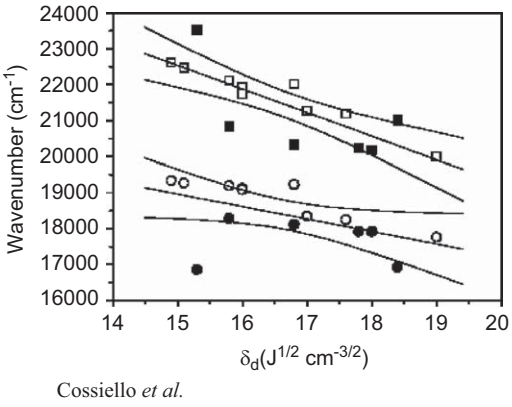

Fig. 11. Energy for the absorption and emission maxima of MEH–PPV in solution of different solvents as a function of the Hildebrandt's dispersion parameter, δ_d. Upper curves and squares: absorption data. Lower curves and circles: emission data. Hollow symbols are data from Ref. [66] and filled symbols are data from this work. Values for toluene and chloroform from both sources coincide. Linear regression line and 95% confidence limits are shown for each correlation.

direction of dichloromethane, THF and toluene. Emission spectra are also quite similar in the three films, with a slight bathochromic shift (1 nm) in the series toluene, dichloromethane and THF. The emission spectra show absence of the α-phase emission, as reported by several authors [13,14,62].

The emission spectra show a slight change with emission wavelength; a decrease in the tendency in the contribution of the 438 nm maximum with respect to the 465 nm one is noted upon with increase in the excitation wavelength (see Fig. 4 in Supporting Information). This behavior parallels that in solution and is a consequence of increased absorption of the β-phase component with increase in the excitation wavelength [63].

The emission spectra in the solid state highly resemble the emission obtained for the f_2 component (β phase), by spectral deconvolution of the steady-state spectra using the wavelength-dependent total anisotropy (Fig. 8).

The steady-state excitation and emission anisotropies of PF films spun from THF solution are shown in Fig. 10 (similar results in films spun from dichloromethane and from toluene solutions are displayed in Fig. 5 of the Supporting Information). The values are quite low, very similar, and they show practically no dependence with wavelength in all films, either in excitation or in emission. Any variation tendency is here within the experimental uncertainty in $\langle r \rangle$ determination of ± 0.02. The low values of the steady-state anisotropy in the solid phase point to a very fast pooling of the electronic excitation energy prior to emission. The facts that $\langle r \rangle$ values are lower in films than those for the α phase in solution, they are wavelength-independent and there is no emission originated in the α phase in the films, all indicate complete energy transfer to the β phase prior to emission, contrary to what is observed in dilute solution. Evidently, the molecular proximity in the solid state is responsible for this fact.

4. Discussion

The absorption spectra of MEH–PPV show a great difference in acetonitrile (the worst solvent used) in comparison with other solvents. The absorption at 425 nm reflects the chain collapse in acetonitrile [64]. The spectral shift in other solvents can be attributed to different amount of isolated and aggregated intrachain chromophores and solvatochromic effects [31,65,66]. Emission spectra show bands corresponding to these two species. No other emitting species is observed due to excitation at 495 nm, where the weak luminescent interchain aggregates do not appreciably absorb [56].

In most cases, preferential solvation has been analyzed in terms of planarity [20,23–25] instead of solubility parameters or other representations of polymer/solvent interactions [46,48–53]. Here we analyze the solvent quality in terms of the components of the Hildebrand solubility parameters for all solvents [50–53]. By comparing these components with profiles of the emission spectra, we conclude that good solvents for MEH–PPV show values of the dispersive and dipolar components in the range $16.8 \leq \delta_d \leq 18.0\ J^{1/2}\ cm^{-3/2}$ and $1.4 \leq \delta_p \leq 5.7\ J^{1/2}\ cm^{-3/2}$, respectively [50–53]. Solvents such as toluene, chloroform and THF have δ_d and δ_p within these ranges while ethyl acetate has a dipolar component as large as δ_p=15.8 $J^{1/2}\ cm^{-3/2}$. Nevertheless, these four solvents have the global solubility parameter in the range 18.7–18.2 $J^{1/2}\ cm^{-3/2}$, which evidences the failure of the global Hildebrand parameters to explain the MEH–PPV solubility differences observed in these solvents. On the other hand, matching of dispersive and dipolar components adequately describes the solubility. In addition, both acetonitrile (δ_d=15.3 $J^{1/2}\ cm^{-3/2}$, δ_p=18.0 $J^{1/2}\ cm^{-3/2}$) and DMSO (δ_d=18.4 $J^{1/2}\ cm^{-3/2}$, δ_p=16.4 $J^{1/2}\ cm^{-3/2}$) have the Hildebrand solubility parameters out of the range adequate for a good solubility of MEH–PPV, which was estimated in a previous work to be 18.7 $J^{1/2}\ cm^{-3/2}$[46]. From the knowledge of the experimental range of the Hansen's parameter [53–55], we estimate the partial solubility parameters for the MEH–PPV as δ_d=18.0 $J^{1/2}\ cm^{-3/2}$, δ_p=4.0 $J^{1/2}\ cm^{-3/2}$, δ_H=3.0 $J^{1/2}\ cm^{-3/2}$ and δ=18.7 $J^{1/2}\ cm^{-3/2}$.

Absorption and emission maxima show a good correlation with the Hildebrandt's dispersion component, as observed in Fig. 11. Correlation with polarity, hydrogen bonding and the total Hildebrandt solubility parameters are definitely uncorrelated (see Supporting information). Data obtained in this work are integrated with literature data, with which they perfectly match [66].

Values for acetonitrile in absorption and in emission as well as data for DMSO in emission fall quite apart from the correlation because the spectroscopically active species is not the same as in the other cases. The good correlation with dispersion forces and not with polar or hydrogen bonding components of Hildebrandt's parameters indicate that dispersion is the most determining

interaction that regulates the spectroscopic features of MEH–PPV in solution. The traditional interpretation of solvent shift produced by dispersion interactions is that they shift the energy of electronic states involved in the transitions. In this case, polymer–solvent interactions also change the effective conjugation length [65,67], and thus enhance the energy of the electronic transition.

Films of MEH–PPV deposited from different solvents show exclusively emission from aggregates. There is a gradual change in the spectra that is in contrast with sharp differences observed in the molecular orientation when isolated polymer chains are deposited on glass from dichloromethane or toluene solutions [67]. This difference is easily explained by the effect of chain interactions in compact polymer films compared to isolated molecules. The different spectral distribution displayed in emission can be explained by heterogeneity in chain conformation in solution, which is transferred to the films [65,67].

The absorption and emission spectra of PF show two distinct bands. In absorption a sharp peak around 435 nm and a broader band at ca 400 nm. The emission shows peaks at 420 and 445 nm, and a shoulder at 465 nm. The different nature of the bands can be better distinguished by the steady-state emission and excitation anisotropies. This is the basis of the spectral decomposition shown in Fig. 8. The electronic transitions identified by the squares in Fig. 8 are attributed to the α phase [13,14,41–43,45,59,60,62], whereas the ones identified by the circles are attributed to the β phase [13,14,41–43,45,59,60,62]. The consistency of the spectra derived in different media and their agreement with published data, validates the analysis. The tendency of fluorescence anisotropy with excitation wavelength was reported previously [45].

We have shown here that the photoluminescence features of MEH–PPV in solution can be explained by solute solvent dispersion interactions. For PF in solution we have shown that the absorption and emission spectra of α and β chains can be separated using the steady-state anisotropy. For both polymers, the spectral features in films are dependent on the chain conformation in the solvent from which they were spun, as already reported in the literature.

To discuss the changes in the steady-state anisotropy in solutions and in thin films, we must consider the polymer properties such as rotational correlation time of the polymer chain, the fluorescence lifetime, the efficiency of the energy migration, the efficiency of the conformational relaxation and the energy transfer processes of the electronic excited states [9,13,14,18–20,23–26,34,41–43,47,55,56,58,59]. All these processes can contribute to the decay in the steady-state anisotropy. Molecular relaxation is expected to play a minor role in rigid luminophores with parallel absorption and emission dipoles. Indeed this is the case in conjugated polymers that have a maximum anisotropy close to 0.4 as in the case of both MEH–PPV and PF [9,13,14,18–20,23–26,34,41–43,47,55,56,58,59]. Conformational relaxation was demonstrated to be only partially responsible for depolarization of fluorene oligomers and depolarization after excitation in the red-edge of the absorption spectrum [18,39,40,43,44,47,59,61]. Furthermore, conformational relaxation is expected to play a still minor role in the depolarization of the conjugated and more rigid MEH–PPV [16,18,21,22,25,26,28,30,32,36].

Molecular rotation is the other parameter that contributes to depolarization if it can take place with comparable rate or faster than the decay of the excited state. Molecular rotation is excluded for the conjugated polymers studied here. On one hand, the polymers have a sub-nanosecond excited state lifetime. On the other hand, 1 ns is approximately the rotational correlation time of a 30 nm^3 molecule (ca. 10 monomer units either of PF or of MEH–PPV) in a 1 mPa s viscous medium at 300 K. Therefore, the rotational correlation time of both, MEH–PPV and PF surely exceeds a value of various ns in solvents used and rotation is discarded in films.

Anisotropy depolarization by energy migration was measured in various conjugated polymers [39,56]. It has a very fast component (<50 ps), accounting for most of the depolarization (from the maximum value of 0.4–0.35 to a value near 0.15), and a slower component (ca. 100 ps) with a small contribution to the depolarization and a residual value of the anisotropy in the range 0.05–0.1 [31,55]. This residual value is higher for stiffer polymer backbones, accounting for the fact that almost parallel energy migration does not contribute to depolarization [68]. For example, the energy migration in MEH–PPV is approximately three times faster than in polythiophenes due to the disordered chain conformation in MEH–PPV and it plays an important role on the anisotropy depolarization [38]. Nevertheless, in the case of PF, although energy migration is an important pathway for the anisotropy depolarization, some anisotropy remains even in the solid state, which means that the energy migration and other energy transfer processes are not totally efficient [39,40,42,44,47,59].

When we compare the anisotropy in solutions and in the solid state there is a remarkable increase in the depolarization of MEH–PPV emission on moving from poor solvents (DMSO and acetonitrile) to polymer films, independently of the solvent (Table 1). Aggregation decreases $\langle r \rangle$ for MEH–PPV either in poor solvents or in films. Because the rotation and conformational relaxation do not play any important role under these conditions, the fluorescence depolarization should be more important due to the greater efficiency of the interchain and intersegmental energy transfer. Therefore, regardless of which MEH–PPV system we analyze (solution or films), fast energy migration/energy transfer processes are always efficient and consequently its anisotropy depolarization is very effective.

The behavior of the PF anisotropy is different compared to MEH–PPV. In this system, the α and the β phases behave quite different; while the homo energy transfer between α segments highly depolarizes its emission, the same homo transfer within the β phase is quite ineffective. Furthermore, the additivity of anisotropy accounts for the observed wavelength dependence of this parameter in excitation and in emission. This additivity means that the two chain conformations behave independent of each other with respect to the electronic energy relaxation, evidencing the lack of energy transfer between them. There is a remarkable coincidence between the excitation and emission spectra of the high anisotropy component and the spectrum of the β phase reported in the literature [60]. These spectroscopic evidences confirm the ordered structure of the β phase, and the lack of electronic energy exchange with the α phase in solution. Finally, the anisotropy in films is almost independent of the solvent quality and there is a very effective energy transfer from the α to the β phases (Table 1).

Acknowledgements

TDZA and RFC thank FAPESP, MCT/CNPq/INEO, CAPES and FAEPEX/Unicamp for financial support and fellowships. PFA is a member of Carrera del Investigador Científico (Research Staff) from CONICET (Consejo Nacional de Investigaciones Científicas y Técnicas, Argentina) and thanks support by grants PIP 5470 (CONICET), PICT 10621 (ANPCyT, Argentina), X086 (UBA), and CAPGBA03/02 (Brazil-Argentina).

Appendix A. Supplementary material

Supplementary data associated with this article can be found in the online version at doi:10.1016/j.jlumin.2009.10.006.

References

[1] S. Miyate, H.S. Nalva, in: Organic Electroluminescent Materials and Devices, , 1998.
[2] J.H. Burroughes, D.D.C. Bradley, A.R. Brown, R.N. Marks, K. Mackay, R.H. Friend, P.L. Burns, A.B. Holmes., Nature 347 (6293) (1990) 539.
[3] L. Akcelrud., Prog. Polym. Sci. 28 (6) (2003) 875.
[4] A.M. Machado, J.D.D. Neto, R.F. Cossiello, T.D.Z. Atvars, L. Ding, F.E. Karasz, L. Akcelrud, Polymer 46 (8) (2005) 2452.
[5] A.M. Machado, M. Munaro, T.D. Martins, L.Y.A. Davila, R. Giro, M.J. Caldas, T.D.Z. Atvars, L.C. Akcelrud, Macromolecules 39 (9) (2006) 3398.
[6] S.H. Yang, C.F.J. Lee., Optoelectron. Adv. Mater. 9 (4) (2007) 2078.
[7] L.H. Chang, Y.D. Lee, C.T. Chen, Macromolecules 39 (9) (2006) 3262.
[8] H.A. Zhang, Y. Li, Q. Jinag, M.G. Xie, J.B. Peng, Y. Cao., J. Mater. Sci. 42 (12) (2007) 4476.
[9] M.B. Ramey, J.A. Hiller, M.F. Rubner, C.Y Tan, K.S. Schanze, J.R. Reynolds, Macromolecules 38 (2) (2005) 234.
[10] Z. Gu, Y.-J. Bao, Y. Zhang, M. Wang, Q.-D. Shen, Macromolecules 39 (9) (2006) 3125.
[11] E.E. Nesterov, Z.G. Zhu, T.M. Swager., J. Am. Chem. Soc. 127 (25) (2005) 10083.
[12] J. Gruber, R.W.C. Li, L.H.J.M.C. Aguiar, T.L. Garcia, H.P.M. Oliveira, T.D.Z. Atvars, A.F. Nogueira., Synth. Met. 156 (24) (2006) 104.
[13] U. Scherf, D. Neher (Eds.), Polyfluorenes Adv. Polym. Sci., vol. 212, Springer-Verlag, Berlin, 2008.
[14] U. Scherf, E.J.W. List., Adv. Mater. 14 (7) (2002) 477.
[15] T. Kawase, T. Shimoda, C. Newsome, H. Sirringhaus, R.H. Friend., Thin Solid Films. 438 (2003) 279.
[16] E.E. Gurel, Y. Pang, F.E. Karasz., Thin Solid Films. 417 (1–2) (2002) 147.
[17] S.R. Amrutha, M.J. Jayakannan., Phys. Chem. B 110 (9) (2006) 4083.
[18] R. Deans, J. Kim, M.R. Machacek, T.M. Swager., J. Am. Chem. Soc. 122 (35) (2000) 8565.
[19] D.T. McQuade, J. Kim, T.M. Swager., J. Am. Chem. Soc. 122 (24) (2000) 5885.
[20] B.J. Schwartz., Ann. Rev. Phys. Chem. 54 (2003) 141.
[21] T. Zyung, S.D. Jung, D.H. Hwang., Synth. Met. 117 (1-3) (2001) 223.
[22] S. Lee, J.Y. Lee, H. Lee., Synth. Met. 101 (1–3) (1999) 248.
[23] T.Q. Nguyen, R.Y. Yee, B.J. Schwartz., J. Photochem. Photobiol. A: Chem. 144 (1) (2001) 21.
[24] T.Q. Nguyen, B.J. Schwartz, R.D. Schaller, J.C. Johnson, L.F. Lee, L.H. Haber, R.J. Saykally., J. Phys. Chem. B 105 (22) (2001) 5153.
[25] R.D. Schaller, L.F. Lee, J.C. Johnson, L.H. Haber, R.J. Saykally, J. Vieceli, I. Benjamin, T.Q. Nguyen, B.J. Schwartz., J. Phys. Chem. B 106 (37) (2002) 9496.
[26] U. Jeng, C.H. Hsu, H.S. Sheu, H.Y. Lee, A.R. Inigo, H.C. Chiu, W.S. Fann, S.H. Chen, A.C. Su, T.L. Lin, K.Y. Peng, S.A. Chen, Macromolecules 38 (15) (2005) 6566.
[27] C.Y. Yang, F. Hide, M.A. Díaz-García, A.J. Heeger, Y. Cao, Polymer 39 (11) (1998) 2299.
[28] J. Teetsov, D.A.V. Bout., J. Phys. Chem. B 104 (40) (2000) 9378.
[29] C.R. McNeill, H. Frohne, J.L. Holdsworth, P.C. Dastoor., Nano Lett. 4 (12) (2004) 2503.
[30] V. Cimrova, D. Neher., Synth. Met. 76 (1–3) (1996) 125.
[31] T.Q. Nguyen, V. Doan, B.J. Schwartz., J. Chem. Phys. 110 (8) (1999) 4068.
[32] D.Y. Kim, J.K. Grey, P.F. Barbara., Synth. Met. 156 (2–4) (2006) 336.
[33] T. Huser, M. Yan, J. Photochem. Photobiol. A: Chem 144 (1) (2001) 43.
[34] S.S. Sartori, S. De Feyter, J. Hofkens, M. Van der Auweraer, F. De Schryver, K. Brunner, J.W. Hofstraat, Macromolecules 36 (2) (2003) 500.
[35] S.H. Chen, A.C. Su, Y.F. Huang, C.H. Su, G.Y. Peng, S.A. Chen, Macromolecules 35 (11) (2002) 4229.
[36] I. Soutar, C. Jones, D.M. Lucas, L. Swanson., J. Photochem. Photobiol. A: Chem. 102 (1) (1996) 87.
[37] K.M. Gaab, C.J. Bardeen., J. Phys. Chem. A 108 (49) (2004) 10801.
[38] A. Synak, G. Gondek, P. Bojarski, L. Kulak, A. Kubicki, M. Szabelski, P. Kwiek., Chem. Phys. Lett. 399 (1–3) (2004) 114.
[39] M. Hennecke, T. Damerau, K. Müllen, Macromolecules 26 (13) (1993) 3411.
[40] L.M. Herz, R.T. Phillips., Phys. Rev. 61 (20) (2000) 13691.
[41] F.B. Dias, A.L. Maçanita, J.S. Melo, H.D. Burrows, R. Günter, U. Scherf, A.P. Monkman., J. Chem. Phys. 39 (15) (2003) 7119.
[42] F.B. Dias, J. Morgado, A.L. Maçanita, P.C. Costa, H.D. Burrows, A.P. Monkman, Macromolecules 39 (17) (2006) 5854.
[43] M. Grell, D.D.C. Bradley, G. Ungar, J. Hill, K.S. Whitehead, Macromolecules 32 (18) (1999) 5810.
[44] A.J. Cadby, P.A. Lane, H. Mellor, S.J. Martin, M. Grell, C. Giebeler, D.D.C. Bradley, M. Wohlgenannt, C. An, Z.V. Vardeny., Phys. Rev. B 62 (23) (2000) 15604.
[45] H.L. Vaughan, F.M.B. Dias, A.P. Monkman., J. Chem. Phys. 122 (1) (2005) 014902.
[46] R.F. Cossiello, L. Akcelrud, T.D.Z. Atvars., J. Braz., Chem. Soc. 16 (1) (2005) 74.
[47] G. Fytas, H.G. Nothofer, U. Scherf, D. Vlassopoulos, G. Meier, Macromolecules 35 (2) (2002) 481.
[48] M.L. Winnik., Photophysical and Photochemical Tools in Polymer Science, vol. 182, D. Riedel, New York, 1986.
[49] J.L. Halary, L. Monnerie., Photophysical and Photochemical Tools in Polymer Science, vol. 182, D. Riedel, New York, 1986, p. 589.
[50] M.H. Hansen.Ind. Eng. Chem. Prod. Res. Dev. 8 (1969) 2.
[51] A.F.M. Barton, in: Handbook of Solubility Parameters and Other Cohesion Parameters, CRC Press, Boca Raton, Florida, 1983, p. 232.
[52] A.F.M. Barton., Chem. Rev. 75 (6) (1975) 731.
[53] J. Brandrup, E.H. Immergut, E.A. Grulke, in: Polymer Handbook, Fourth ed., Academic Press, New York, 1993, p. 2336.
[54] M.M.L. Grage, P.W. Wood, A. Ruseckas, T. Pullerits, W. Mitchell, P.L. Burn, I.D.W. Samuel, V. Sundstrom., J. Chem. Phys. 118 (16) (2003) 7644.
[55] C.J. Collison, L.J. Rothberg, V. Treemaneekarn, Y. Li, Macromolecules 34 (7) (2001) 2346.
[56] U. Lemmer, S. Heun, R.F. Mahrt, U. Scherf, M. Hopmeier, U. Siegner, E.O. Gobel, K. Mullen, H. Bässler., Chem. Phys. Lett. 240 (4) (1995) 373.
[57] J.R. Lakowicz, in: Principles of Fluorescence Spectroscopy, Academic Press, New York, 1999.
[58] S.H. Chen, A.C. Su, C.H. Su, S.A. Chen, Macromolecules 38 (2) (2005) 379.
[59] S.H. Chen, H.L. Chou, A.C. Su, S.A. Chen, Macromolecules 37 (18) (2004) 6833.
[60] M.J. Winokur, J. Slinker, D.L. Huber., Phys. Rev. B 67 (18) (2003) 184106.
[61] J.G. Müller, E. Atas, C. Tan, K.S. Schanze, V.D. Kleiman., J. Am. Chem. Soc. 128 (12) (2006) 4007.
[62] D. Marushchak, L.B.A. Johansson., J. Fluorescence 15 (5) (2005) 797.
[63] H. Azuma, K. Asada, T. Kobayashi, H. Naito., Thin Solid Films 509 (1–2) (2006) 182.
[64] H.Z. Tang, M. Fujiki, M. Motonaga, Polymer 43 (23) (2002) 6213.
[65] R. Traiphol, N. Charoenthai, T. Srikhirin, T. Kerdcharoen, T. Osotchan, T. Maturos, Polymer 48 (3) (2007) 813.
[66] O. Narwark, S.C.J. Meskers, R. Peetz, E. Thorn-Csányi, H. Bässler., Chem. Phys. 294 (1) (2003) 1.
[67] S. Quan, F. Teng, Z. Xu, L. Qian, Y. Hou, Y. Wang, X. Xu., Eur. Polym. J. 42 (1) (2006) 228.
[68] R. Traiphol, P. Sanguansat, T. Srikhirin, T. Kerdcharoen, T. Osotchan, Macromolecules 42 (20) (2006) 1165.